Physica E 76 (2016) 140–145

Contents lists available at ScienceDirect

Physica E

journal homepage: www.elsevier.com/locate/physe

Effect of strain-polarization fields on optical transitions in AlGaN/GaN multi-quantum well structures

V. Kladko [a], A. Kuchuk [a,b,*], A. Naumov [a], N. Safriuk [a], O. Kolomys [a], S. Kryvyi [a], H. Stanchu [a], A. Belyaev [a], V. Strelchuk [a], B. Yavich [c], Yu.I. Mazur [b], M.E. Ware [b], G.J. Salamo [b]

[a] V. Lashkaryov Institute of Semiconductor Physics, National Academy of Sciences of Ukraine, Pr. Nauky 45, Kyiv 03028, Ukraine
[b] Institute for Nanoscience and Engineering, University of Arkansas, W. Dickson 731, 72701 Fayetteville, USA
[c] JSC "Svetlana Optoelectronica", Engelsa ave. 47, Saint-Petersburg 194156, Russia

HIGHLIGHTS

- The influence of strain on optical transitions in Al0.1Ga0.9N/GaN MQWs was studied.
- Strain in the buffer leads to the equal sign deformation in the well and the barrier.
- Polarization fields cause a strong separation of the confined electrons and holes.
- DAP's recombination dominates over electron-hole states transitions in the QW.

ARTICLE INFO

Article history:
Received 5 August 2015
Received in revised form
19 October 2015
Accepted 20 October 2015
Available online 23 October 2015

Keywords:
AlGaN/GaN
Multi-quantum well
Deformation state
Piezoelectric field
Photoluminescence
X-ray diffraction

ABSTRACT

The influence of strain and barrier/well thickness ratio on recombination processes in multi-quantum well (MQW) $Al_{0.1}Ga_{0.9}N$/GaN structures was investigated using X-ray diffraction and Raman and photoluminescence spectroscopies. The deformation state of the wells and barriers was determined. In addition, the value of the polarization fields, the density of polarization charges, and the positions of energy levels for optical transitions within the quantum wells were calculated. It was established that compressive strain in the buffer layer as well as in the layers of the MQWs with respect to the buffer layer lead to the piezoelectric fields having equal sign in the well and the barrier. As a result, the recombination of donor–acceptor pairs dominates over transitions between electron and hole states in the quantum well.

1. Introduction

In recent years, the effect of built-in electric fields in hexagonal III-nitrides has gained the attention of researchers in the nitrides community. Due to the non-centrosymmetric structure of the hexagonal III-nitrides, there is a spontaneous polarization present in the bulk [1–4]. In addition, when fabricating strained heterostructures of AlGaN/GaN or InGaN/GaN, the effect of piezoelectric polarization has to be taken into account [5,6]. Both the spontaneous and the piezoelectric polarizations give rise to a large built-in field that has implications for both optical and electronic device design. Such a built-in electric field causes: (i) band bending and red-shift of the gap, which largely overcomes the blue-shift expected from quantum size effects, and, (ii) a progressive separation of the electron and hole wave functions with increasing well width, resulting in the decrease of the emission strength and of the exciton binding energy [7]. The total polarization of the material ultimately depends on several factors, which can be controlled during epitaxial growth opening the way for polarization engineering in III-nitride based electronics.

The influence of strain on the local polarization-induced electric fields and the subsequent effect on the energy levels in $Al_xGa_{1-x}N$/GaN multi-quantum wells (MQWs) and superlattices (SL) has been studied in [8–11]. Additionally, experimental observations of the dependence of a two dimensional hole gas density on the thickness and/or alloy composition and resulting strain variation of an AlGaN barrier were studied in [12]. Moreover, the effect of strain and polarization fields on phonon modes complicates the interpretation of the vibrational spectrum of the $Al_xGa_{1-x}N$/GaN SL. In [13] the change in phonon spectrum of AlN/

* Corresponding author at: V. Lashkaryov Institute of Semiconductor Physics, National Academy of Sciences of Ukraine, Pr. Nauky 45, Kyiv 03028, Ukraine.
E-mail address: kuchuk@uark.edu (A. Kuchuk).

http://dx.doi.org/10.1016/j.physe.2015.10.022
1386-9477/

GaN SLs with different well-to barrier ratio and in-plane strain was analyzed, and the strain-free frequencies of the SL modes were estimated. Thus, to obtain the predicted optimization of parameters for light emitting nitride heterostructures one requires a detailed understanding of the influence of elastic deformation and the relaxation mechanism on the polarization effect. It should be noted that the selection of the appropriate thickness and composition is also very important.

In this work we investigated the nature of the emission bands in the AlGaN/GaN MQWs as the ratio between the well and the barrier thickness changes. In addition, the values of the elastic deformation in the layers of the $Al_{0.1}Ga_{0.9}N$/GaN heterostructures were obtained. Polarization fields, density of polarization charge, and the position of the energy bands for optical transitions were calculated.

2. Experimental

Multi-quantum well structures formed by 10-periods of $Al_xGa_{1-x}N$/GaN grown by MOCVD were investigated in this work. The growth started with a 3.5 μm Si doped GaN buffer layer. This was grown on a 0.5 μm GaN layer with intrinsic conductivity, which was grown on a 20 nm low temperature nucleation GaN layer on a *c*-plane sapphire substrate. The first sample, S1, consisted of 7 nm $Al_xGa_{1-x}N$ barriers with $x=0.1$ and 10 nm GaN QWs. The second sample, S2, consisted of 13.2 nm $Al_xGa_{1-x}N$ barriers with $x=0.1$ and 5.5 nm GaN QWs. Thicknesses and composition were calculated from X-ray diffraction data.

X-ray investigations were carried out using a high resolution X'Pert PRO MRD diffractometer from PANalytical. The reciprocal space map (RSM) and diffraction rocking curves (RC) were obtained in a triple-axis configuration and were used to determine the structural parameters. The strain in the GaN buffer layers was directly calculated from the experimental 2θ-ω scans which were referenced to the (0006) reflection of the sapphire substrate. Theoretical diffraction rocking curves were calculated using the methods described in Refs. [14,15]. Material parameters used in this work were taken from [16,17]. Low temperature micro-photoluminescence and Raman spectra were obtained using a Horiba–Jobin Yvon T64000 triple spectrometer with a CCD detector and an Olympus BX41 confocal microscope (object lens NUV × 40, NA=0.4). Optical spectra were excited by a He–Cd laser with the photon energy $h\nu=3.81$ eV (13 mW) and Ar–Kr laser with the photon energy $h\nu=2.54$ eV (50 mW). The excitation power was varied in a wide range using neutral density filters.

3. Results and discussion

Reciprocal space mapping (RSM) is a powerful tool to study the structural quality, composition, and deformation state of an epitaxial layer. From asymmetrical RSMs, the in- and out-of-plane lattice parameters of the individual layers can be extracted. Thus, to get information about the relaxation level, i.e. the deformation state of our films, the asymmetric RSMs around the (-1-124) GaN reflection for samples S1 and S2 were measured and analyzed as described previously [15,18–20]. As seen in Fig. 1, these RSMs show the GaN buffer layer as the large central spot with a nearly vertically aligned column of satellites from the $Al_xGa_{1-x}N$/GaN MQWs. The observed small displacement along the Q_x coordinate between this vertical column of MQW peaks and the GaN spot indicates a partial relaxation at this interface, i.e. there is a small change in the average in-plane lattice constants between the GaN and the MQW ($a_{GaN}\neq a_{MQW}$). For S1 $a_{GaN}=3.1871\pm0.0005$ Å, $a_{MQW}=3.1874\pm0.001$ Å and for S2 $a_{GaN}=3.1871\pm0.0005$ Å, $a_{MQW}=3.1881\pm0.001$ Å). We find a slightly larger relaxation value in S1 ($r=4.7\%$) than in S2 ($r=3.7\%$), where $r=(a_{MQW}-a_{GaN})^{exp}/(a_{MQW}-a_{GaN})^{teor}$. However, the presence of satellites indicates a high degree of coherence remaining in the MQW with respect to the buffer layer.

It is interesting to note that the position of the GaN peaks on the RSMs indicates that the buffer is in a compressive state, i.e. not fully relaxed. This is confirmed by careful comparison with the (0006) sapphire substrate peak in symmetric 0002 $2\theta/\omega$ scans (not shown). This is expected from the lattice constant of the *c*-plane sapphire substrate and the natural 30° twist of the GaN unit cell with respect to that substrate [21].

More precise analysis of the structural parameters of the $Al_xGa_{1-x}N$/GaN MQWs was provided by modeling the experimental diffraction rocking curve from the (0002) symmetric reflection (see Fig. 2). Following the method described previously [18–20], we used dynamical diffraction theory and the deformation parameters of the layers received from the RSMs. It can be seen from the inset of Fig. 2b that the angular position and the intensity of the thickness oscillations in the calculated curves agree very well with those of the experimental curves. Structure parameters obtained from the RSM and refined by fitting the experimental curves are tabulated in the inset of Fig. 2. According to these results, both layers of the MQW (the well and the barrier) are compressed; however the compressive deformation in the GaN layers is larger than in $Al_{0.1}Ga_{0.9}N$ layers. Moreover, the difference in strain between samples S1 and S2 can be attributed to changes in the average of the lattice parameter of the MQW period ($\langle a_{MQW}$

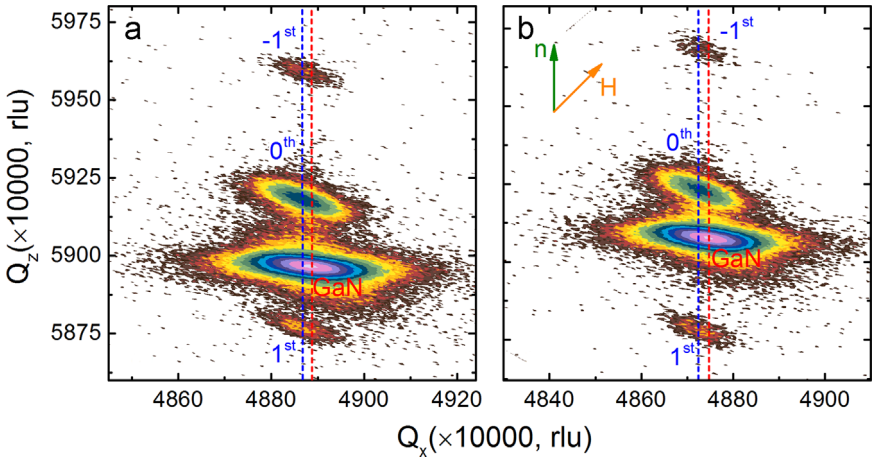

Fig. 1. RSMs in the vicinity of the (-1-124) reflection for the AlGaN/GaN MQWs: (a) S1 and (b) S2. Q_z and Q_x – reciprocal lattice coordinate, perpendicular and parallel to the surface. ***H*** – diffraction vector, ***n*** – vector of surface normal.

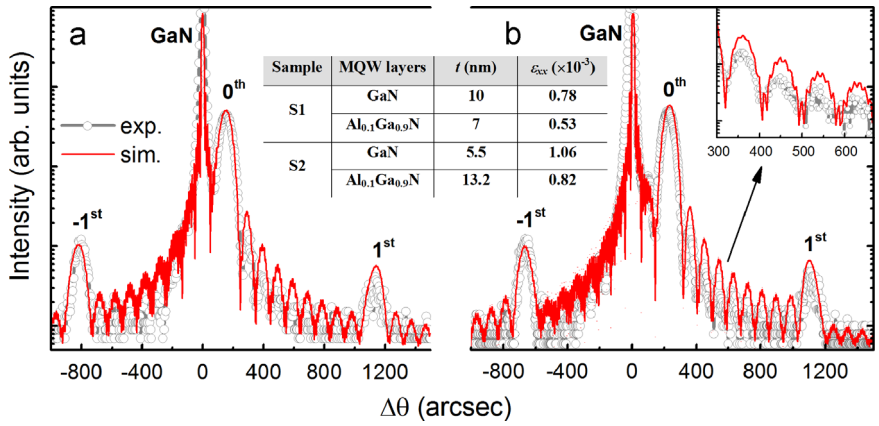

Sample	MQW layers	t (nm)	ε_{xx} ($\times 10^{-3}$)
S1	GaN	10	0.78
	$Al_{0.1}Ga_{0.9}N$	7	0.53
S2	GaN	5.5	1.06
	$Al_{0.1}Ga_{0.9}N$	13.2	0.82

Fig. 2. $2\theta/\omega$-scans for symmetrical reflex (0002) from the AlGaN/GaN MQW: (a) S1 and (b) S2. Experiment – black curve, fitting – red curve. (For interpretation of the references to color in this figure legend, the reader is referred to the web version of this article.)

$\rangle=(a_w t_w+a_b t_b)/(t_w+t_b)$), caused by the difference in the ratio of the thickness of the well to that of the barrier (t_w/t_b).

In order to verify the data obtained from the XRD studies the structures were additionally investigated using Raman scattering and photoluminescence experiments. Fig. 3a shows low-temperature resonant Raman spectra (RS) of the two different $Al_{0.1}Ga_{0.9}N$/GaN MQW samples using laser excitation with energy, $E_{ex}=3.81$ eV, just above the fundamental absorption edge of GaN. Due to the absorption of this energy light dominant contribution to the RS is from the MQW layer not the buffer layer [22]. Due to the near resonance conditions for the AlGaN and GaN epilayers i.e., as the incident laser energy approaches the energies of the crystal intermediate states, the intensity of the LO modes are strongly enhanced via the Fröhlich interaction. In addition, the changing confined intersubband states between samples S1 and S2 result in different resonant conditions for the RS which result in different enhancements in the two samples. The most prominent peaks in the RS are from LO modes (A_1^{LO}) of AlGaN and GaN epilayers. The E_2 (high) nonpolar Raman modes from the GaN are also visible at 569 cm^{-1}.

Assuming a solid solution of $Al_xGa_{1-x}N$ the frequency of the A_1^{LO} phonon has a single mode character [23]. For unstrained $Al_xGa_{1-x}N$ this is given by equation $\omega_{A_1^{LO}} = 746 + 169.5x + 11.7x^2 - 36.6x^3$ [24], which results in a value of 766.0 cm^{-1} for $x=0.1$ ($T=90$ K). This region of the spectra is shown in Fig. 3a along with the A_1^{LO} modes for both GaN and AlGaN and their fits using Lorenzian profiles. From these fits we can estimate the frequencies to be $\omega_{A_1^{LO}}(Al_{0.1}Ga_{0.9}N) \approx 769.3$ cm^{-1} for sample S1 with the thin barrier (7 nm) and $\omega_{A_1^{LO}}(Al_{0.1}Ga_{0.9}N) \approx 767.3$ cm^{-1} for sample S2 with the thick barrier (13 nm). Similarly, we see the GaN A_1^{LO} frequency shift away from its unstrained value of 737.0 cm^{-1}. For sample S1 $\omega_{A_1^{LO}}$(GaN) ≈ 739.1 cm^{-1}, and for sample S2 $\omega_{A_1^{LO}}(GaN) \approx 740.2$ cm^{-1}. In both cases the observed frequency shift of the A_1^{LO} phonon is caused by the presence of lateral compressive strain.

Fig. 3b shows room temperature nonresonant Raman spectra of the samples AlGaN/GaN MQWs for thickness ratio barrier/well 7/10 nm (curve S1) and 13/5.5 nm (curve S2) under a 2.54 eV excitation far from resonant conditions. So the Raman scattering information is mainly from the thick GaN buffer layer because the visible light can penetrate the whole AlGaN/GaN MQWs. The Raman scattering signals from thin AlGaN barrier layer and GaN spacer layer has weak intensity. Therefore, Raman spectra shown two signatures corresponding to the E_2(high) and A_1(LO) modes of the GaN thick buffer layer for the samples S1 and S2 which are located at 569.7 and 569.2 cm^{-1}, 735.9 and 736.0 cm^{-1}, respectively. Estimations of biaxial strain in the growth plane of the structure are carried out from the position of the E_2 (high) phonon mode using the relation $\Delta\omega=\omega-\omega_0=K(E_2(\text{high}))\sigma$, where $\omega_0=567.6$ cm^{-1}, $K(E_2(\text{high}))=-2.7$ cm^{-1}/GPa [25]. As can be seen from Fig. 3b (inset), the GaN buffer layers are strained with compressive deformation up to 0.78 GPa and 0.59 GPa for S1 and S2 samples, respectively. Thus, micro-Raman investigations confirm the XRD results that the thick buffers GaN as well as both layers of MQW structures are under compression.

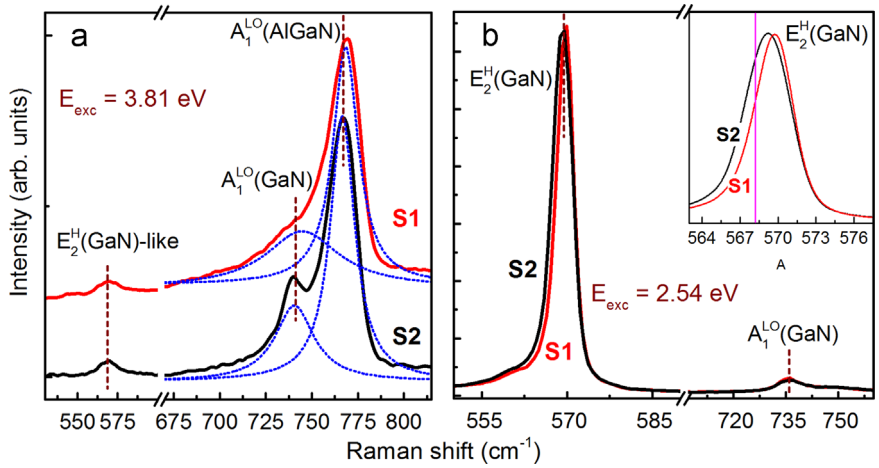

Fig. 3. Resonant ($E_{ex}=3.81$ eV) (a) and nonresonant ($E_{ex}=2.54$ eV) (b) Raman spectra of AlGaN/GaN MQWs for thickness ratio barrier/well 7/10 nm (curve S1) and 13/5.5 nm (curve S2).

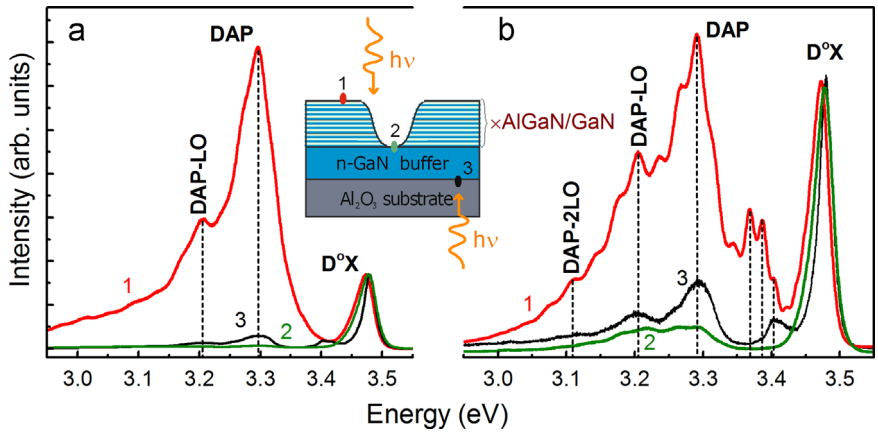

Fig. 4. PL spectra for MQW samples (a) S1 with a well to barrier thickness ratio of 10/7 and (b) S2 with a ratio of 5.5/13. Numbers in scheme of the etched AlGaN/GaN MQW sample correspond the curve labels in (a) and (b). E_{exc}=3.81 eV, T=83 K. P_{exc}=2.0 W/cm^2.

Additionally, photoluminescence (PL) spectroscopy was used for characterization of the $Al_xGa_{1-x}N$/GaN MQW structures. Earlier, the efficiency of such PL measurements to establish the nature of radiative recombination of a 2DEG with holes in modulation-doped $Al_xGa_{1-x}N$/GaN structures was demonstrated [26]. In order to investigate the nature of optical radiation bands with energy lower than the band gap E_g(GaN) we etched the $Al_xGa_{1-x}N$/GaN MQW layers using reactive ion etching to reach the thick n-GaN buffer layer. The depth of the etched conical pit was estimated to be 300–400 nm. The PL spectra obtained are shown in Figs. 4a and b for samples S1 and S2, respectively. The label on each spectral curve corresponds to the numbers in the inset of Fig. 4 describing the different configuration of the PL excitation and collection. For these spectra we used E_{ex}=3.81 eV and P_{ex}=2.0 W/cm^2 for the excitation energy and power density, respectively. Curve 1 represents the spectra of the un-etched material. Curve 2 represents the spectra from inside the etched pit, i.e. the PL of the doped GaN buffer. And, curves 3 are the PL spectra from the thick GaN buffer layer exited through the back side of the Al_2O_3 substrates. Taking into account the value of absorption coefficient $\alpha=(1.2–1.5)\times 10^5$ cm^{-1} in GaN [27], the photoexcited carriers are efficiently created only in about 0.1-μm-thick region of the surface layer. Thus, for point #1 the MQW region is excited, while for points #2 and #3 0.1-μm region of the surface buffer GaN layer from face- and back-side, is excited, respectively.

The radiative recombination mechanism in AlGaN/GaN MQWs is generally considered to be excitonic in undoped samples [28]. In the exciton range of the PL spectrum from the $Al_xGa_{1-x}N$/GaN MQWs (curve 1) we observed the presence of an intense near-band-edge emission band peak at about 3.47 eV ($\Gamma\approx 35$ meV), originating from the neutral donor-bound exciton recombination (D°X) in the GaN layer (typically observed in HEMT structures) [29]. The low-energy shoulder of the D°X band at about $h\nu$=3.43–3.46 eV is assigned to recombination involving electrons from the 2DEG at the GaN/AlGaN heterointerface and photoexcited free holes in the GaN layer [30,31]. We do not observe the so-called free A- excitons (FE) at 3478 eV [27], because the D°X band is much broader than the energy distance between the energy maximum of D°X and the FE bands. Furthermore, as seen from Fig. 4b, for the S2 sample another additional band including three PL peaks at 3.402, 3.368 eV and 3.385 eV are visible. These peaks, observed at low temperature, we attribute to electron–hole recombination in the QWs. The bands disappear after etching of MQW samples (curve 2 on Fig. 4) which proves their relation to transitions between free carriers in QWs.

A detailed analysis of the nature of these QW bands is uncertain due to overlap of probably inequivalent PL spectra from the different active quantum wells in the $Al_xGa_{1-x}N$/GaN MQWs samples. An alternative explanation would be a local variation in well widths in the near surface region.

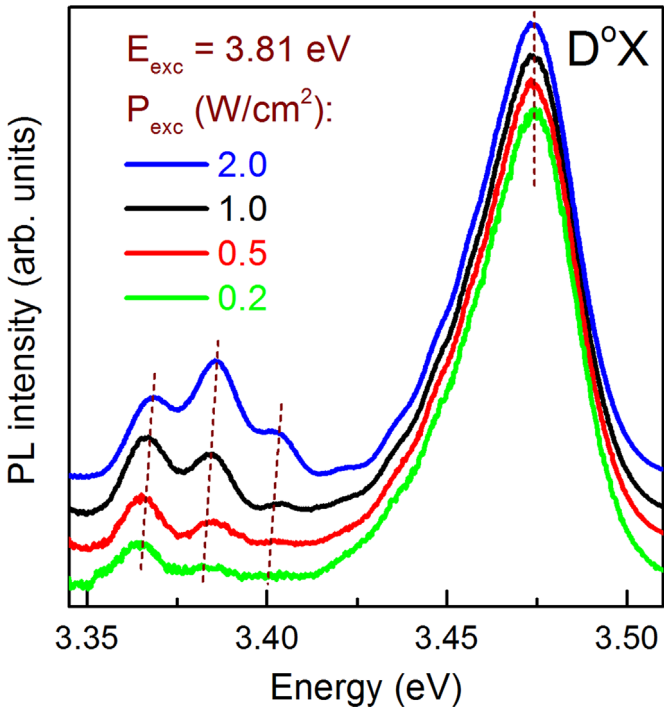

Fig. 5. Excitation-power-dependent PL spectra for sample S2. E_{exc}=3.81 eV, T=83 K.

The power dependence of PL intensity allows us to additionally investigate the nature of these bands. Fig. 5 shows the near-band-edge PL spectra of sample S2 measured with varying excitation powers. This shows that the D°X peak does not shift with increasing excitation intensity. But, when excitation power intensity is increased, the enhanced steady-state concentration of excess carriers results in reduced bending of the conduction band at the heterointerface due to increased carrier screening. Thus, the triangular potential well in the conduction band edge at the heterointerface also becomes shallower. And, a blue shift of the QWs peaks is observed with increasing excitation intensity. Note that the intensity of this QWs PL peaks decreases with increasing temperature and they disappear at ~120 K.

When we changed the position of the excitation point from the bottom of the pit on the n-GaN buffer layer to the surface, the D°X

Table 1
Spontaneous and piezoelectric charges (P_{sp},P_{pz}), and built-in electric field (F^w) in MQW's layers.

Samples	MQW layers	P_{sp} (C/m^2)	P_{pz} (C/m^2)	F^w (V/m)
S1	GaN	-3.4×10^{-2}	-0.73×10^{-3}	2.83×10^{7}
	AlGaN	-3.96×10^{-2}	-0.538×10^{-3}	
S2	GaN	-3.4×10^{-2}	-0.99×10^{-3}	4.9×10^{7}
	AlGaN	-3.96×10^{-2}	-0.83×10^{-3}	

band shifted gradually to lower energy by ≈ 9 meV. Similar energy shifts due to residual strain in GaN epilayers grown on sapphire have been previously observed [30,31]. It is known that the GaN layers are biaxially strained during the high temperature growth and cool down due to the difference in thermal expansion coefficients between the GaN and the sapphire. This low energy strain-induced shift of the D^{o}X band is the subsequent result of relaxation of the compressive strain introduced in the GaN as the thickness increases. Using the energy position of the D^{o}X band in comparison with that in bulk GaN allows for the estimation of the biaxial strain value in the GaN layer. In [32] it was shown that, the energy shift of the PL emission band is related to strain by the equation $\Delta E=0.141\times\Delta\varepsilon_c$, where ΔE is the difference of optical transition energy and $\Delta\varepsilon_c$ is the difference in strain along c-axis. Therefore, if the entire ~9 meV energy shift is caused by strain there is a corresponding change in strain value of $\Delta\varepsilon_c=0.064\%$ in the GaN layers of the studied samples.

Also in the micro-PL spectra from the two $Al_xGa_{1-x}N$/GaN MQWs we observed the broad emission band at ~3.26–3.29 eV, with a FWHM of 80 ± 1 meV, which appears to be due to the donor–acceptor pair (DAP) recombination in GaN, which involves the shallow donor responsible for the residual n-type conductivity and a shallow acceptor not clearly identified. A strong DAP emission intensity is normally caused by a high concentration of intrinsic acceptors. For GaN, V_{Ga} or C_N are often considered as probable acceptors [33]. Fig. 4b shows also apparent DAP bands with LO-phonon replicas (LO-phonon energy is $h\nu_{LO}\approx90$ meV) appeared in the PL spectra of sample S2. The presence of phonon replicas may indicate the extent of crystal lattice ordering and strong interaction between local electrons and phonons.

The intensity of the electron–hole recombination band at 3.402–3.385 eV in the case of sample S2 is significantly lower than intensity of the DAP recombination due to weak overlapping of the electron and hole envelope wave functions in the QWs. In the case of the sample S1 the QW is thick enough such that there was no significant overlap of the electron and hole envelope wave functions. Thus, the corresponding electron–hole transitions are not observed. To confirm this we modeled the energy band structure in our MQWs samples. First, we calculated the polarization charges and the built-in electric field in the quantum well using polarization theory equations [4,34] and the experimental data on the deformation, ε_{xx}, obtained from the RSM. The characteristic material parameters of the AlGaN alloy were determined as a linear combination of those of AlN and GaN. The values of the spontaneous polarization, elastic and piezoelectric constants were taken from [33,35]. Finally, because all layers are under compressive stress, we take the spontaneous polarization and piezoelectric fields to point in the same direction in these layers. The results of these calculations are given in Table 1.

Then, solving Poisson's and Schrödinger equations self-consistently and taking into account the calculated values of the polarization fields we modeled the band structure and confined energy levels in the $Al_xGa_{1-x}N$/GaN MQWs. From this we can estimate the lowest energy PL peak position for electron–hole recombination in the QWs to be 3.35 eV to 3.40 eV for S1 and S2, respectively. These model estimations obtained using experimental values from RSM agree well with optical experiment and observed PL band at 3.402–3.385 eV for S2. Indeed, calculated values of electric fields in QWs are sufficient to cause a very strong carrier separation. As one can see from Fig. 6 overlapping of the electron and the hole envelope functions becomes very small in the case of sample S2 resulting in a low intensity of electron–hole recombination. This recombination practically vanishes in the case of sample S1 due to the ten times less overlapping than for S2.

4. Conclusions

The structural and optical properties of $Al_{0.1}Ga_{0.9}N$/GaN MQWs were studied using X-ray diffraction and optical techniques. It was

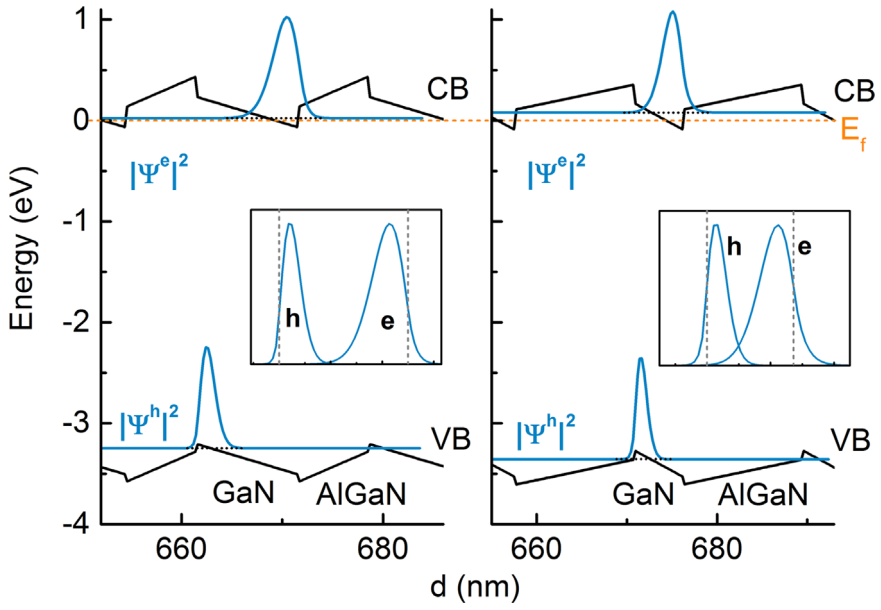

Fig. 6. Band diagram and squares of the envelope functions for the conduction-band electrons and the valence-band heavy holes within 10 nm (S1) and 5.5 nm (S2) GaN quantum wells including polarization. E_f-Fermi level. For simulating of band structure and energy levels we used the nextnano software [36].

established that strong compressive strain in the buffer layers as well as in the layers of a MQW with a low content of Al in the barrier will lead to a situation where piezoelectric fields have equal sign in the well and the barrier. The possibility to govern this value and direction of polarization opens the way for polarization engineering in III-nitride based electronics. We can predict that control of the level of strain in templates and in the layers of a MQW can create equal and opposite spontaneous and piezoelectric polarization, for example, to achieve a similar result to using non-polar planes.

Acknowledgments

This study was supported by the National Academy of Sciences of Ukraine within the state program “Nanotechnology and Nanomaterials”.

References

[1] H. Morkoç, Handbook of Nitride Semiconductors and Devices: Electronic and Optical Processes in Nitrides, Wiley–VCH, Berlin, 2008.
[2] P.P. Paskov, J.P. Bergman, V. Darakchieva, T. Paskova, B. Monemar, M. Iwaya, S. Kamiyama, H. Amano, I. Akasaki, Photoluminescence of GaN/AlN superlattices grown by MOCVD, Phys. Status Solidi C 2 (2005) 2345–2348.
[3] B.K. Ridley, W.J. Schaff, L.F. Eastman, Theoretical model for polarization superlattices: energy levels and intersubband transitions, J. Appl. Phys. 94 (2003) 3972–3978.
[4] S.H. Park, S.L. Chuang, Spontaneous polarization effects in wurtzite GaN/AlGaN quantum wells and comparison with experiment, Appl. Phys. Lett. 76 (2000) 1981–1983.
[5] P. Perlin, C. Kisielowski, V. Iota, B.A. Weinstein, L. Mattos, N.A. Shapiro, J. Kruger, E.R. Weber, J. Yang, InGaN/GaN quantum wells studied by high pressure, variable temperature, and excitation power spectroscopy, Appl. Phys. Lett. 73 (1998) 2778–2780.
[6] J. Kudrna, P.G. Gucciardi, A. Vinattieri, M. Colocci, B. Damilano, F. Semond, N. Grandjean, J. Massies, Steady-state and time-resolved near-field optical spectroscopy of GaN/AlN quantum dots and InGaN/GaN quantum wells, Phys. Status Solidi A 190 (2002) 155–160.
[7] G. Traetta, A. Passaseo, M. Longo, D. Cannoletta, R. Cingolani, M. Lomascolo, A. Bonfiglio, A. Di Carlo, F. Della Sala, P. Lugli, A. Botchkarev, H. Morkoç, Effects of the spontaneous polarization and piezoelectric felds on the luminescence spectra of $Al_{0.26}Ga_{0.74}N$ quantum wells, Physica E 7 (2000) 929–933.
[8] B. Jogai, J.D. Albrecht, E. Pan, Energy levels in polarization superlattices: a comparison of continuum strain models, Semicond. Sci. Technol. 19 (2004) 733–741.
[9] A. Atsushi Yamaguchi, Valence band engineering for remarkable enhancement of surface emission in AlGaN deep-ultraviolet light emitting diodes, Phys. Status Solidi C. 5 (2008) 2364–2366.
[10] D.Y. Fu, R. Zhang, B.G. Wang, B. Liu, Z.L. Xie, X.Q. Xiu, H. Lu, Y.D. Zheng, G. Edwards, Biaxial and uniaxial strain effects on the ultraviolet emission efficiencies of $Al_xGa_{1-x}N$ films with different Al concentrations, J. Appl. Phys. 108 (2010) 103107.
[11] S. Fan, Z. Qin, C. He, X. Wang, B. Shen, G. Zhang, Strain effect on the optical polarization properties of *c*-plane $Al_{0.2}6Ga_{0.74}N$/GaN superlattices, Opt. Express 22 (2014) 6322–6328.
[12] M.S. Shur, A.D. Bykhovsky, R. Gaska, Two-dimensional hole gas induced by piezoelectric and pyroelectric charges, Solid-State Electron. 44 (2000) 205–210.
[13] V. Darakchieva, E. Valcheva, P.P. Paskov, M. Schubert, T. Paskova, B. Monemar, H. Amano, I. Akasaki, Phonon mode behavior in strained wurtzite AlN/GaN superlattices, Phys. Rev. B 71 (2005) 115329.
[14] O.M. Yefanov, V.P. Kladko, The solution of the dispersion equation in an explicit format for a case of two strong waves, Metallofiz. Nov. Tekh. 28 (2006) 227–244 (in Russian).
[15] V.P. Kladko, A.V. Kuchuk, N.V. Safryuk, V.F. Machulin, P.M. Lytvyn, V. G. Raicheva, A.E. Belyaev, Yu.I. Mazur, E.A. DeCuir Jr, M.E. Ware, M. O. Manasreh, G.J. Salamo, Influence of template type and buffer strain on structural properties of GaN multilayer quantum wells grown by PAMBE, an X-ray study, J. Phys. D.: Appl. Phys. 44 (2011) 025403.
[16] N.V. Safriuk, G.V. Stanchu, A.V. Kuchuk, V.P. Kladko, A.E. Belyaev, V.F. Machulin, X-ray diffraction investigation of GaN layers on Si(111) and Al_2O_3(0001) substrates, SPQEO 16 (2013) 265–272.
[17] M.A. Moram, M.E. Vickers, X-ray diffraction of III-nitrides, Rep. Prog. Phys. 72 (2009) 036502.
[18] V. Kladko, A. Kuchuk, P. Lytvyn, O. Yefanov, N. Safriuk, A. Belyaev, Yu.I. Mazur, E.A. DeCuir Jr, M.E. Ware, G.J. Salamo, Substrate effects on the strain relaxation in GaN/AlN short-period superlattices, Nanoscale Res. Lett. 7 (2012) 289.
[19] A.V. Kuchuk, V.P. Kladko, T.L. Petrenko, V.P. Bryksa, A.E. Belyaev, Yu. I. Mazur, M.E. Ware, E.A. DeCuir Jr, G.J. Salamo, Mechanism of strain influenced quantum well thickness reduction in GaN/AlN short-period superlattices, Nanotechnology 25 (2014) 245602.
[20] V.P. Kladko, A.F. Kolomys, M.V. Slobodian, V.V. Strelchuk, V.G. Raycheva, A. E. Belyaev, S.S. Bukalov, H. Hardtdegen, V.A. Sydoruk, N. Klein, S.A. Vitusevich, Internal strains and crystal structure of the layers in AlGaN/GaN heterostructures grown on a sapphire substrate, J. Appl. Phys. 105 (2009) 063515.
[21] V.P. Kladko, A.V. Kuchuk, N.V. Safryuk, V.F. Machulin, A.E. Belyaev, H. Hardtdegen, S.A. Vitusievich, Mechanism of strain relaxation by twisted nanocolumns revealed in AlGaN/GaN heterostructures, Appl. Phys. Lett. 95 (2009) 031907.
[22] J.F. Muth, J.H. Lee, I.K. Shmagin, R.M. Kolbas, H.C. Casey Jr., B.P. Keller, U. K. Mishra, S.P. DenBaars, Absorption coefficient, energy gap, exciton binding energy, and recombination lifetime of GaN obtained from transmission measurements, Appl. Phys. Lett. 71 (1997) 2572–2574.
[23] V.Yu Davydov, I.N. Goncharuk, A.N. Smirnov, A.E. Nikolaev, W.V. Lundin, A. S. Usikov, A.A. Klochikhin, J. Aderhold, J. Graul, O. Semchinova, H. Harima, Composition dependence of optical phonon energies and Raman line broadening in hexagonal $Al_xGa_{1-x}N$ alloys, Phys. Rev. B 65 (2002) 125203.
[24] M. Kuball, Raman spectroscopy of GaN, AlGaN and AlN for process and growth monitoring/control, Surf. Interface Anal. 31 (2001) 987–999.
[25] H. Harima, Properties of GaN and related compounds studied by means of Raman scattering, J. Phys.: Condens. Matter 14 (2002) R967.
[26] T. Wang, J. Bai, S. Sakai, Modulation-doping influence on the photoluminescence from the two-dimensional electron gas of $Al_xGa_{1-x}N$/GaN heterostructures, Phys. Rev. B 63 (2001) 205320.
[27] Michael A. Reshchikov, Hadis Morkoç, Luminescence properties of defects in GaN, J. Appl. Phys. 97 (2005) 061301.
[28] I. Friel, C. Thomidis, Y. Fedyunin, T.D. Moustakas, Investigation of excitons in AlGaN/GaN MQW by lateral photocurrent and PL ss, J. Appl. Phys. 95 (2004) 3495.
[29] W. Rieger, T. Metzger, H. Angerer, R. Dimitrov, O. Ambacher, M. Stutzmann, Influence of substrate-induced biaxial compressive stress on the optical properties of thin GaN films, Appl. Phys. Lett. 68 (1996) 970.
[30] W. Shan, T.J. Schmidt, X.H. Yang, S.J. Hwang, J.J. Song, B. Goldenberg, Temperature dependence of interband transitions in GaN grown by MOCVD, Appl. Phys. Lett. 66 (1995) 985.
[31] C.I. Harris, B. Monemar, H. Amano, I. Akasaki, Exciton lifetimes in GaN and GaInN, Appl. Phys. Lett. 67 (1995) 840.
[32] S.W. Lee, Jun-Seok Ha, Hyun-Jae Lee, Lee Hyo-Jong, H. Goto, T. Hanada, T. Goto, Katsushi Fujii, M.W. Cho, T. Yao, Lattice strain in bulk GaN epilayers grown on CrN/Sapphire substrate, Appl. Phys. Lett. 94 (2009) 082105.
[33] Monemar, Luminescence in III-nitrides, Mater. Sci. Eng. 59 (1999) 122–132.
[34] O. Ambacher, J. Majewski, C. Miskys, A. Link, M. Hermann, M. Eickhoff, M. Stutzmann, F. Bernardini, V. Fiorentini, V. Tilak, B. Schaff, L.F. Eastman, Pyroelectric properties of Al(In)GaN/GaN hetero- and quantum well structures, J. Phys. Condens. Matter, 14, (2002) 3399–3434.
[35] F. Bernardini, V. Fiorentini, D. Vanderbilt, Spontaneous polarization and piezoelectric constants of III–V nitrides, Phys. Rev. B 56 (1997) R10024.
[36] StefanBirner, Nextnano GmbH/www.nextnano.com.